THE JOURNAL OF BIOLOGICAL CHEMISTRY VOL. 282, NO. 37, pp. 26997–27005, September 14, 2007

Live Cell FRET Microscopy

*HOMO- AND HETERODIMERIZATION OF TWO HUMAN PEROXISOMAL ABC TRANSPORTERS, THE ADRENOLEUKODYSTROPHY PROTEIN (ALDP, ABCD1) AND PMP70 (ABCD3)**

Received for publication, March 12, 2007, and in revised form, June 26, 2007 Published, JBC Papers in Press, July 3, 2007, DOI 10.1074/jbc.M702122200

Merle Hillebrand[‡1], Sophie E. Verrier[§], Andreas Ohlenbusch[‡], Annika Schäfer[‡], Hans-Dieter Söling[§†], Fred S. Wouters[¶], and Jutta Gärtner[‡1]

From the [‡]Department of Pediatrics and Pediatric Neurology, Georg August University, Faculty of Medicine, Robert-Koch-Strasse 40, 37075 Göttingen, Germany, the [§]Department of Neurobiology, Max Planck Institute of Biophysical Chemistry, Am Fassberg 11, 37077 Göttingen, Germany, and the [¶]Cell Biophysics Group, European Neuroscience Institute, Waldweg 33, 37073 Göttingen, Germany

The adrenoleukodystrophy protein (ALDP) and the 70-kDa peroxisomal membrane protein (PMP70) are half-ATP-binding cassette (ABC) transporters in the mammalian peroxisome membrane. Mutations in the gene encoding ALDP result in a devastating neurodegenerative disorder, X-linked adrenoleukodystrophy (X-ALD) that is associated with elevated levels of very long chain fatty acids because of impaired peroxisomal β-oxidation. The interactions of peroxisomal ABC transporters, their role in the peroxisomal membrane, and their functions in disease pathogenesis are poorly understood. Studies on ABC transporters revealed that half-transporters have to dimerize to gain functionality. So far, conflicting observations are described for ALDP. By the use of *in vitro* methods (yeast two-hybrid and immunoprecipitation assays) on the one hand, it was shown that ALDP can form homodimers as well as heterodimers with PMP70 and ALDR, while on the other hand, it was demonstrated that ALDP and PMP70 exclusively homodimerize. To circumvent the problems of artificial interactions due to biochemical sample preparation *in vitro*, we investigated protein-protein interaction of ALDP in its physiological environment by FRET microscopy in intact living cells. The statistical relevance of FRET data was determined in two different ways using probability distribution shift analysis and Kolmogorov-Smirnov statistics. We demonstrate *in vivo* that ALDP and PMP70 form homodimers as well as ALDP/PMP70 heterodimers where ALDP homodimers predominate. Using C-terminal deletion constructs of ALDP, we demonstrate that the last 87 C-terminal amino acids harbor the most important protein domain mediating these interactions, and that the N-terminal transmembrane region of ALDP has an additional stabilization effect on ALDP homodimers. Loss of ALDP homo- or heterodimerization is highly relevant for understanding the disease mechanisms of X-ALD.

The adrenoleukodystrophy protein (ALDP,[2] ABCD1) is a member of the ATP-binding cassette (ABC) transporter protein family, and one of four ABC transporters in the mammalian peroxisomal membrane. The other members are the adrenoleukodystrophy-related protein (ALDR, ABCD2), the 70-kDa peroxisomal membrane protein (PMP70, ABCD3), and the PMP70-related protein (P70R/PMP69, ABCD4) (1–6).

Mutations in the gene encoding ALDP cause X-linked adrenoleukodystrophy (X-ALD), the most common inherited peroxisomal disorder that is characterized by the abnormal accumulation of saturated very long chain fatty acids (VLCFAs) predominantly in brain white matter, adrenal cortex, and testis (7–10). The clinical phenotype is highly variable ranging from the devastating childhood cerebral form with progressive demyelination to the existence of asymptomatic individuals. The pathogenesis of X-ALD and especially the exact function of peroxisomal ABC transporters in the disease process are still completely unknown. ALDP and the other peroxisomal ABC transporters may be involved in the import of VLCFAs or activated fatty acids across the peroxisomal membrane into the peroxisomal lumen for degradation (11, 12) as described for the yeast peroxisomal ABC homologs Pxa1 and Pxa2 also called Pat1 and Pat2 (13, 14).

Localization of the ABC transporters to the peroxisomal membrane is mediated by Pex19p (15, 16). The known targeting motif for peroxisomal localization is at the N-terminal part of ABC transporters. For ALDP AA68–82 function as binding site for Pex19p. In addition, two membrane domains are necessary for correct intracellular localization (17, 16). AA 1–124 are required for peroxisomal localization of PMP70, and the binding site for Pex19p is included in the first 60 AA (18, 19, 20).

ABC transporters generally consist of two homologous halves, each containing a membrane-spanning domain with multiple hydrophobic transmembrane helices and a hydro-

* This work was supported by Deutsche Forschungsgemeinschaft (DFG) Grant Ga 354/4-1 (to J. G.) and by the DFG Research Center for Molecular Physiology of the Brain (to F. S. W.). The costs of publication of this article were defrayed in part by the payment of page charges. This article must therefore be hereby marked "*advertisement*" in accordance with 18 U.S.C. Section 1734 solely to indicate this fact.

† Professor Dieter Söling died on March 6th, 2006.

[1] To whom correspondence should be addressed. Tel.: 49-551-398035; Fax: 49-551-396252; E-mail: gaertnj@med.uni-goettingen.de.

[2] The abbreviations used are: ALDP, adrenoleukodystrophy protein; FRET, Förster resonance energy transfer; ABC, ATP-binding cassette; ALDR, adrenoleukodystrophy-related protein; PMP70, 70-kDa peroxisomal membrane protein; P70R, PMP70-related protein; X-ALD, X-linked adrenoleukodystrophy; VLCFA, very long chain fatty acid; NBF, nucleotide binding fold; AA, amino acid; ECFP, enhanced cyan fluorescent protein; EYFP, enhanced yellow fluorescent protein; PDF, probability density function; CDF, cumulative density function; KS, Kolmogorov-Smirnov.

TABLE 1

Oligonucleotide sequences used for construction of plasmids

Oligonucleotide sequences are shown from 5′- to 3′-end. Restriction sites in the sequence of the cloning oligonucleotides are shown in italics and restriction enzymes are listed.

Name	Sequence (5′–3′)	Restriction enzyme
ALDP up	tta*ctcgag*caatgccggtgctctccaggccccgg	XhoI
ALDP down	ttt*aagctt*tcaggtggaggcaccctggaggcc	HindIII
ALDP390 down	ttt*aagctt*gttgcgggcaatagtgaaggc	Hin III
ALDP550 down	ttt*aagctt*cacagacatgtagggcctctgcg	HindIII
ALDP658 down	ttt*aagctt*ggtgatggagagcagggcaatgc	HindIII
ALDPdel551–657	aat*acatgt*ctcaccggccctccctgtggaa	PciI
ALDPdelNBF	att*aagctt*caccggccctccctgtggaa	HindIII
ALDPdown without Stop	ttt*aagctt*ggtggaggcaccctggaggcc	HindIII
ALDP-EYFP-N1-Mut for	cagggtgcctccaccaagcttcgaattctg	
ALDP-EYFP-N1-Mut rev	cagaattcgaagcttggtggaggcaccctg	
ALDP-Stop-Del for	ggcctccagggtgcctccaccaagcttcgaattc	
ALDP-Stop-Del rev	gaattcgaagcttggtggaggcaccctggaggcc	
Mut-Pci I for	Gccttttgctcacttgttctttcctgc	
Mut-Pci I rev	gcaggaaagaacaagtgagcaaaaggc	
PMP70-N1 up	taa*ctcgag*atggcggccttcagcaagtacttg	XhoI
PMP70-N1 down	tta*ggatcc*tgagagccaaactcaactgtatc	BamHI
Pex26 for	Tta*ctcgag*caatgaagagcgattcttcg	XhoI
Pex26 rev	Tta*gaattc*tcagtcacggatgcggagc	EcoRI

philic cytosolic nucleotide binding fold (NBF) (21). The NBF contains the highly conserved motifs Walker A, Walker B and 19-mer that are important for substrate specificity and nucleotide binding (22, 23). ABC transporters can either be found as complete full-size transporters comprising twelve transmembrane helices and two NBFs, or as half transporters comprising six transmembrane helices and a single NBF. The multiple drug resistance transporter (MDR) (24) and the cystic fibrosis transmembrane regulator (CFTR) (25) are exemplars for the former, and TAP1 and TAP2 proteins (26) for the latter. All four mammalian peroxisomal ABC transporters known to date belong to the group of ABC half-transporters and thus form obligate homodimers or heterodimers to attain functionality (27). So far, *in vitro* studies for dimerization of peroxisomal ABC transporters have given inconsistent observations. Investigations by three different groups using yeast two-hybrid and co-immunoprecipitation experiments revealed that human ALDP could form either homodimers or heterodimers with PMP70 and ALDR (28–30). These results could not be confirmed by a further investigation using immunoprecipitated ALDP and PMP70 complexes from digitonin-solubilized mouse liver peroxisomes; ALDP as well as PMP70 could only be detected as homomeric proteins and not in heteromeric association (31).

To further elucidate the interaction of ABC transporters in the peroxisomal membrane and especially the formation of homo- or heterodimers for human ALDP and PMP70, we applied FRET microscopy in intact living cells, a method that avoids artificial alterations due to biochemical sample preparation prior to analysis. In addition, we generated various ALDP deletion constructs to identify the protein domains that mediate ALDP dimerization.

EXPERIMENTAL PROCEDURES

Plasmid Constructions—All oligonucleotides used for plasmids constructions are listed in Table 1. The cDNA fragments encoding ALDP, ALDP390 (AA1 to AA390), ALDP550 (AA1 to AA550), ALDP658 (AA1 to AA658), ALDPΔ551–657 (residues 551–657 were deleted), and ALDPΔNBF (residues 391–657 were deleted) (Fig. 1) were amplified from RZPD clone IRAKp961 0514Q2 (Deutsches Ressourcenzentrum für Genomforschung GmbH, Berlin) by PCR. Amplification products were cloned into pECFP-N1, pEYFP-N1, or pECFP-C1 vectors (Clontech) via the corresponding restriction enzymes. The stop codon was deleted from the ALDP constructs by site-directed mutagenesis using the site-directed mutagenesis kit (Stratagene) and the oligonucleotides "ALDP-EYFP-N1-Mut for" and "ALDP-EYFP-N1-Mut rev." ALDPΔ551–657 was constructed as follows: the C-terminal part of ALDP (AA658-AA745) was amplified using the oligonucleotide pair "ALDP down" and "ALDPdel551–657". The PciI restriction site inside the vectors of the ALDP658-ECFP-N1 and ALDP658-EYFP-N1 constructs was disrupted by site-directed mutagenesis using oligonucleotides "Mut-PciI for" and "Mut-PciI rev". Digestion of these constructs with PciI and HindIII resulted in the AA1 to AA551 fragment to which the C-terminal part of ALDP (AA658-AA745) was ligated leading to ALDP missing residues 551 to 657 (Fig. 1). The stop codons were deleted by site-directed mutagenesis PCR with oligonucleotides "ALDP-Stop-Del for" and "ALDP-Stop-Del rev". For the ALDPΔNBF constructs AA 391 to AA 657 were deleted. Therefore, ALDP390 constructs were linearized by HindIII and ligated with the C-terminal part of ALDP (AA658 to AA745) amplified with oligonucleotides ALDPdelNBF and ALDPdown without Stop by PCR. PMP70 was amplified from total human cDNA by PCR using oligonucleotides "PMP70-N1 up" and "PMP70-N1 down." The amplified product was cloned into vectors pECFP-N1 and pEYFP-N1 via the appropriate restriction sites. Pex26, a peroxisomal single transmembrane protein with its N terminus exposed to the cytosol, was amplified from the constructs described by Weller *et al.* (32) using the oligonucleotides "Pex26 for" and "Pex26 rev" and subsequently cloned into vector pECFP-C1. All PCR amplifications except for the mutagenesis were performed using the BD Advantage™ 2 PCR kit (Clontech) according to the manufacturer's recommendations. The identity of all constructs was verified by sequence analysis.

Cell Culture and Electroporation—Either CHO cells or monkey cells are often used for peroxisomal studies. Because an efficient electroporation protocol for VERO cells was estab-

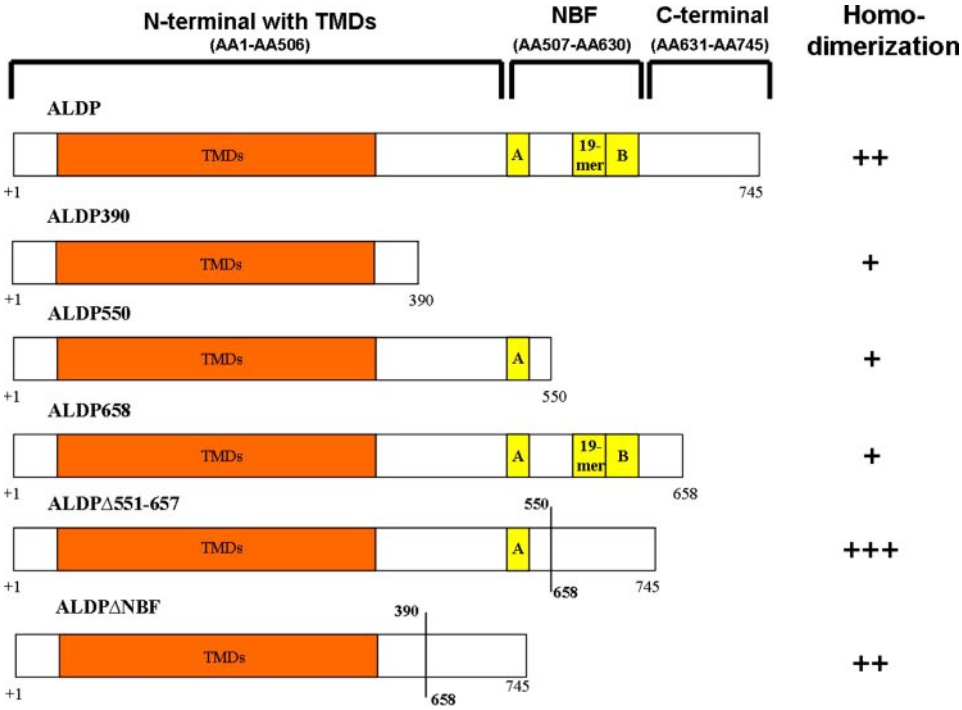

FIGURE 1. **Scheme of ALDP constructs used for FRET experiments.** ALDP constructs used for FRET experiments are shown. The *orange color* represents the transmembrane domains (*TMDs*) consisting of six membrane-passing segments. The Walker A motif (A), the 19-mer sequence (19-mer) also called C-region and the Walker B motif (B) of the NBF are illustrated in *yellow*. Numbers mark amino acid positions. ALDP658, ALDP550, and ALDP390 are truncated at the C terminus. In ALDPΔ551–657 the internal amino acids 551–657 are deleted, while in ALDPΔNBF amino acids 391–657 are deleted. +, ++, and +++ indicate low, moderate, and high FRET, respectively.

lished in our laboratories, we used these cells for the experiments. For cell culture, Vero cells (African green monkey kidney cells, ECACC 84113001) were grown in Dulbecco's modified Eagle's medium (Cambrex) supplemented with 2 mM glutamine, 10% (v/v) heat-inactivated fetal calf serum, 100 units/ml penicillin, 0.1 mg/ml streptomycin at 37 °C and 10% CO_2. At the time of confluency, cells were harvested by trypsinization, washed with phosphate-buffered saline and resuspended in 300 μl of cytomix (120 mM KCl, 10 mM KH_2PO_4, 10 mM K_2HPO_4, 2 mM EGTA, 5 mM $MgCl_2$, 25 mM HEPES, 0.15 mM $CaCl_2$, 5 mM GSH, and 2 mM ATP pH7.4) containing 10 to 15 μg of each DNA coding for the indicated proteins. Immediately thereafter cells were transfected by electroporation (Gene Pulser II, Bio-Rad, pulse 0.7 kV, 50 μF, 1–2 ms) and grown until the experiment.

Live Cell FRET Microscopy Experiments—For single cell FRET experiments, CFP and YFP were used as donor and acceptor fluorescent molecules, respectively. FRET measurements were performed 24 h after electroporation using an inverted microscope (Axiovert200, Zeiss). To minimize organelle movement, cells were cooled down on ice in cold medium prior to measurement. To minimize background fluorescence, the medium HAM's F-12 without phenol red (PromoCell) was used. CFP was detected using a filter set composed of an excitation filter 436/20 nm, a dichroic beam splitter 455 nm and an emission filter 480/40 nm. For YFP an excitation filter 500/20 nm, a dichroic beam splitter 515 nm and an emission filter 535/30 nm were used. The FRET filter set consisted of an excitation filter 436/20 nm, a dichroic beam splitter 455 nm and an emission filter 535/30 nm. Images were acquired using a cooled charge-coupled device camera and the Metamorph 6 software (Universal Imaging Corporation West Chester).

Image Analysis—All image processing was performed using ImageJ. Images were registered for stage translation between acquisitions using the "TurboReg" plugin (P. Thévenaz, Swiss Federal Institute of Technology, Lausanne) converted to 32 bit, binned 2 × 2, and subjected to a median filter with kernel size 0.5. The YFP image intensities were matched to the exposure time of the CFP and FRET images. Background fluorescence was estimated from an area free of cells and subtracted. The spectrally corrected FRET ratio was calculated by Equation 1,

$$\text{FRET ratio} = \frac{\text{FRET} - a \times \text{CFP} - b \times \text{YFP}}{\sqrt{\text{CFP} \times \text{YFP}}} \quad \text{(Eq. 1)}$$

where a and b represent correction factors for YFP and CFP bleed-through emissions into the FRET images, respectively. Note that the equation normalizes the FRET signals to the expression levels of the fluorescent proteins (33). The resulting corrected FRET ratio was multiplied by a digital mask that was generated from an intensity-threshold YFP image of the same sample to remove noise generated by low-intensity regions. All further calculations were performed using the Igor Pro suite (Wavemetrics Inc. Portland, OR). FRET ratio distribution histograms were generated and normalized to unity. Cumulative histograms of experiments on the same conditions were re-normalized to unity to obtain probability density functions (PDF). The PDF of the negative control Pex26 co-expressed with ALDP was fitted with a Gaussian function to obtain the value of the mean + 3× the standard deviation (3σ), corresponding to a FRET ratio of 0.215. For each cell, the probability of exceeding this 3σ threshold, *i.e.* the probability of obtaining FRET ratios higher than contained in the negative control, was obtained by integration of the PDF above the 3σ threshold. The mean probability value for all conditions and their standard error on the mean (S.E.) was subjected to one-way analysis of variance with pair-wise Tukey post-doc testing for statistical significance.

The PDFs were also subjected to statistical testing using the Kolmogorov-Smirnov method that takes into account changes over the entire distribution of FRET ratios per condition. The PDFs were integrated to obtain cumulative density functions (CDFs), and the pair-wise probability for statistically significant differences between conditions was calculated from the CDFs

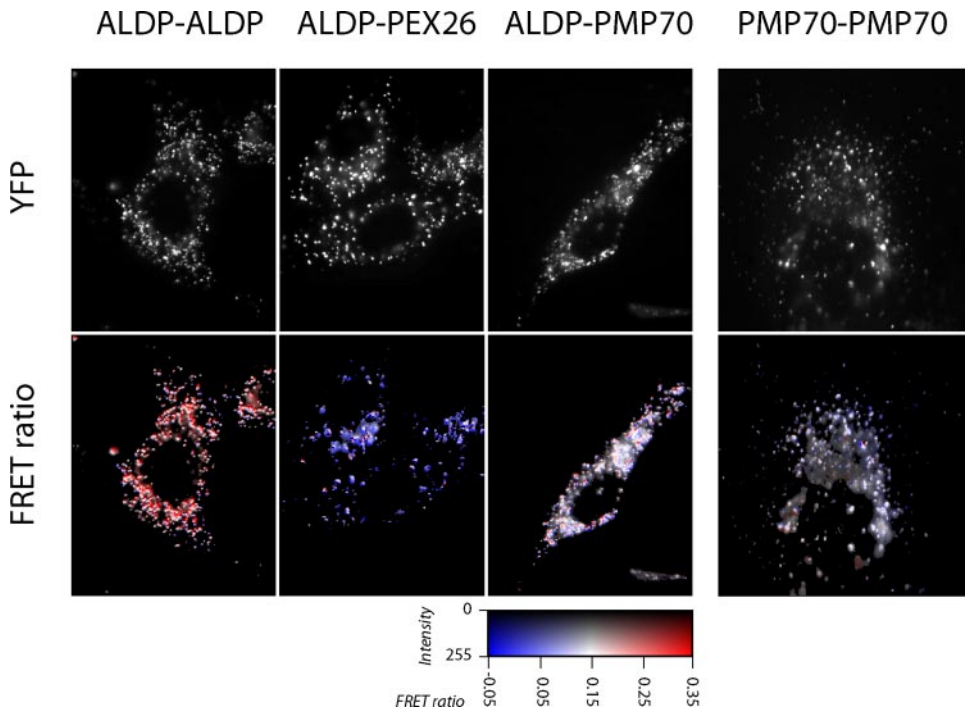

FIGURE 2. **ALDP and PMP70 homodimerization and ALDP/PMP70 heterodimerization.** The *upper panel* shows the fluorescence distribution of ALDP-EYFP in peroxisomes of cells that co-express CFP-labeled ALDP, Pex26, and PMP70 (*left three images*). The localization of the CFP-labeled protein is identical to that of ALDP-EYFP (not shown). The *right image* shows the fluorescence distribution of PMP70-EYFP. Again this signal perfectly co-localizes with the co-expressed PMP70-ECFP. The interaction of the CFP-labeled proteins with ALDP-EYFP (*left three images*) or the homodimerization between EYFP- and ECFP-labeled PMP70 (*right image*), as judged by the presence of FRET is shown in the *lower panel* (for the calculation of the FRET ratio see "Experimental Procedures." The FRET ratio is shown in false color ranging from *blue* (low FRET), via *white* (intermediate FRET) to *red* (high FRET). Color saturation is weighed by the fluorescence intensity of ALDP-EYFP (*left three images*) or PMP70-EYFP (*right image*), *dark colors* correspond to dim structures and *full colors* to bright structures.

using the statistical package of the MatLab suite (The Mathworks, Inc. Natick, MA).

Representative examples of the FRET ratio for different conditions are represented in an intensity-weighed color lookup table where color saturation varies in accordance with the fluorescence intensity of the YFP image.

Comparison of Protein Expression Levels—Expression levels of ALDP and PMP70 were measured by means of fluorescence microscopy on a cell-by-cell basis (38). Cells were transfected with either ALDP-ECFP-N1 or PMP70-ECFP-N1. 24 h after transfection, cells were fixed and stained with either ALDP antibody (ALD-1D6-As or ALD-2B4-As, Euromedex), or PMP70 antibody (kindly provided by Wilhelm Just, Heidelberg). Corresponding Cy3-labeled secondary antibodies were used for visualization (Jackson Laboratories). Intensity differences between transfected (as judged by CFP fluorescence) and untransfected cells were used to determine the relative overexpression level of ALDP or PMP70 (endogenous and transfected protein), according to Equation 2,

$$f = \frac{I - I_0}{I_0} \qquad \text{(Eq. 2)}$$

where f is the fold overexpression relative to endogenous protein, and I and I_0 represent the staining intensities of transfected and untransfected cells in the same field of observation, respectively.

RESULTS

Protein-Protein Interaction of ALDP with ALDP, PMP70, and Pex26 and of PMP70 with PMP70—Because ALDP and PMP70 can only function upon dimerization, we performed FRET measurements in living cells to assess potential interactions *in vivo*. To determine whether ALDP and PMP70 can form heterodimers as described by Liu *et al.* (1999) or function exclusively as a homomeric protein unit as proposed by Guimarães *et al.* (31), we transfected Vero cells with ALDP-EYFP and co-expressed ALDP-ECFP or PMP70-ECFP or transfected cells with PMP70-ECFP and co-expressed PMP70-EYFP. As a negative control, we co-expressed Pex26-ECFP, a peroxisomal membrane protein with a single transmembrane domain that is not related to ABC transporters (34). The proper peroxisomal localization of the fluorescently tagged proteins was verified by single transfection of each construct together with ECFP-SKL or EYFP-SKL, a well established fluorescent peroxisomal marker (data not shown). Because the peroxisomal targeting signal for ABC transporters is located at the N-terminal part while the EYFP/ECFP is located at the C terminus, the tag did not influence localization. In addition, expression of full-length proteins was verified by Western blot analysis (data not shown).

Functionality of the proteins is not impaired by fluorescent protein fusion as shown by ALDR-EGFP that is able to rescue the C26:0 β-oxidation in X-ALD fibroblasts (35).

Fig. 2 shows the peroxisomal localization of the FRET acceptors ALDP-EYFP and PMP70-EYFP. The respective CFP-labeled donor protein revealed complete co-localization (data not shown). The FRET ratios of the expression combinations ALDP-EYFP/ALDP-ECFP, ALDP-EYFP/Pex26-ECFP, ALDP-EYFP/PMP70-ECFP, and PMP70-EYFP/PMP70-ECFP of representative cells 20 to 24 h after transfection are exemplarily shown. The FRET ratio is represented in false colors ranging from blue (low FRET) via white to red (high FRET). Cells co-expressing ALDP-EYFP and ALDP-ECFP show strong FRET with an overall ratio of 0.3 (Fig. 2, *left lower panel*) indicative of efficient homodimerization. The FRET ratio is homogeneously distributed over peroxisomes in the cell. In contrast, co-expression of ALDP-EYFP and Pex26-ECFP does not reveal significant FRET, confirming that ALDP does not interact with peroxisomal membrane proteins in general, and thus the applicability of Pex26 as a negative control. The FRET ratios are homogeneously low (ratio ~0.05; Fig. 2, *lower left middle*

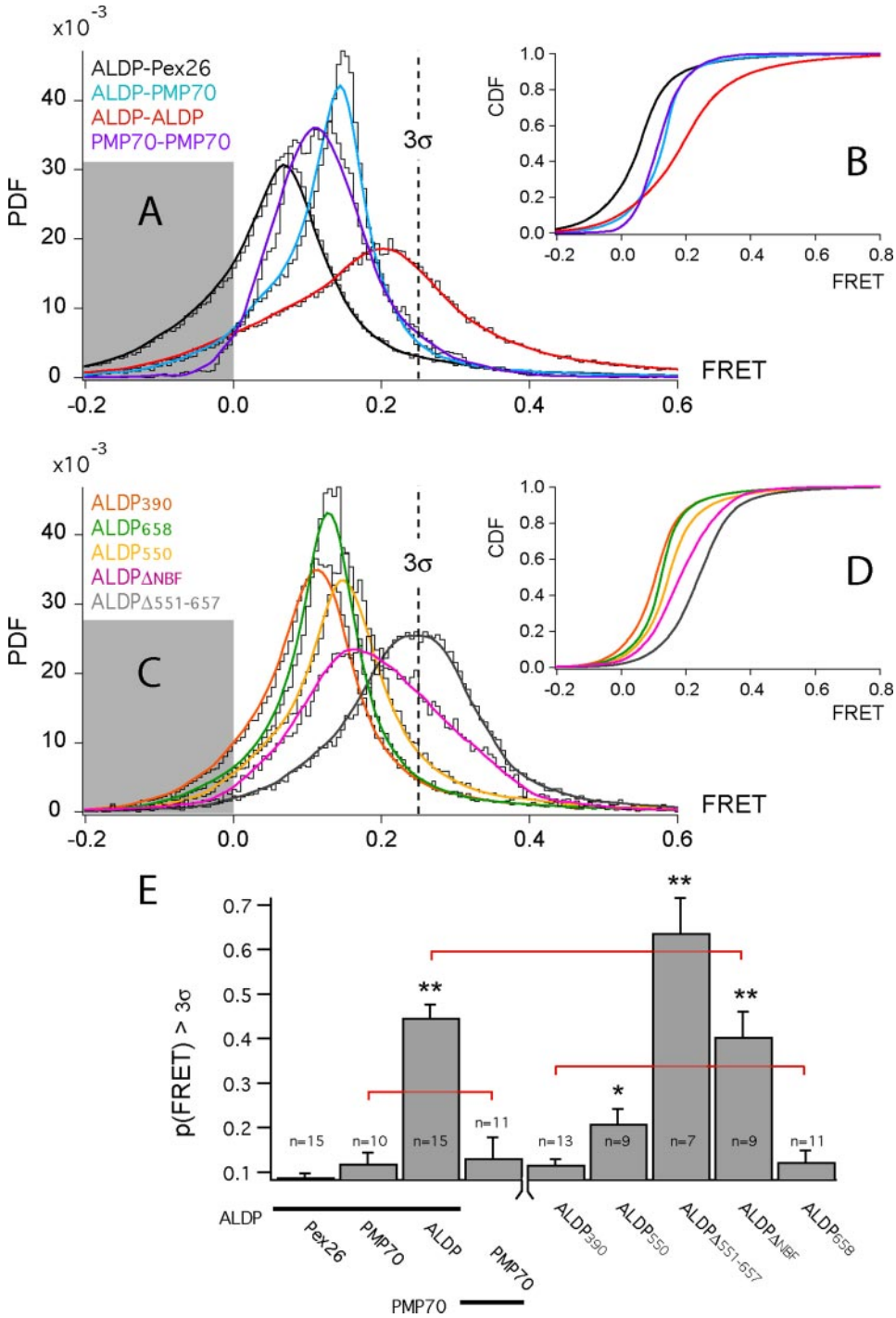

FIGURE 3. **Statistical analysis of protein-protein interactions analyzed by FRET microscopy.** *A*, cumulative normalized and weighed FRET ratio distributions (probability density functions, PDF) of the interaction between ALDP-EYFP and CFP-labeled ALDP (*red trace*, $n = 15$ cells), Pex26 (*black trace*, $n = 15$), and PMP70 (*blue trace*, $n = 10$), and between PMP70-EYFP and PMP70-ECFP (*purple trace*, 11 cells) as shown in Fig. 2. The threshold for the detection of FRET, *i.e.* the average plus three times the standard deviation of ALDP-Pex26 interaction is indicated by a *dashed line* (3σ, equal to a FRET ratio of 0.215). *B*, integrated PDFs, the cumulative density function (*CDF*), of *panel A* using the same color-coding for the different conditions. The probability that traces are different due to chance is calculated by the largest vertical separation between pairs of traces using the Kolmogorov-Smirnov method. *C*, PDFs of the homodimerization of the truncation ALDP mutants ALDP390 (*orange trace*, $n = 13$ cells), ALDP550 (*yellow trace*, $n = 9$), ALDPΔ551–657 (*gray trace*, $n = 7$), ALDPΔNBF (*pink trace*, $n = 9$), and ALDP658 (*green trace*, $n = 11$). The corresponding CDFs are shown in *D* using the same color-coding. *E*, probability of exceeding the threshold FRET ratio for the negative control ALDP-Pex26 was determined for each cell in every condition and is represented in the bar graph as average ± S.E. Statistical significance of deviation from the ALDP-Pex26 interaction is indicated: **, significant at the 5% level; *, significant at the 10% level. Kolmogorov-Smirnov testing was used to test the statistical significance of pair-wise differences between conditions at the 1% level. *Red brackets* show the conditions in *panels A* and *C* that are statistically indistinguishable. All other conditions within the *panels A* and *C* are statistically different.

panel). Co-expression of ALDP-EYFP and PMP70-ECFP results in intermediate FRET with an overall ratio of 0.15 (Fig. 2, *lower right middle panel*). Intermediate FRET can also be seen in cells expressing PMP70-ECFP and PMP70-EYFP. The ratio for these constructs is 0.15 (Fig. 2, *lower right panel*). These data are indicative of the heterodimerization of ALDP and PMP70 and of PMP70 homodimerization, respectively. Although the ratio is lower than that obtained for co-expression of ALDP with itself, it is clearly higher than that obtained for ALDP co-expression with Pex26.

We further confirmed the extent of the revealed protein-protein interactions by quantitative statistical analysis in two different ways. First, using a recently published method (36) suitable for non-Gaussian distributions. Briefly, from the distribution of FRET ratios for the negative control situation ALDP/Pex26, an upper FRET ratio threshold was determined that could still be statistically attributed to the absence of FRET. This threshold was derived by Gaussian fitting of the ALDP/Pex26 distribution, followed by the calculation of the mean ratio plus three times the standard deviation. This value corresponded to a FRET ratio of 0.215 and was used as reference for all other FRET measurements. The occurrence of FRET in cells was defined as a significant increase in the probability of exceeding this threshold, namely in obtaining values larger than 0.215. This probability can be estimated by normalization of the integral of the FRET ratio distribution of each cell to unity (yielding the so-called probability density function, PDF). The integral of the PDF bins exceeding the threshold represents the probability of detecting significant FRET. By performing this analysis on 15 ALDP/Pex26, 10 ALDP/PMP70, 15 ALDP/ALDP, and 11 PMP70/PMP70 co-expressing cells, the mean probability and its standard error on the mean was obtained. The results are shown in the first four bars of *panel E* in Fig. 3. The

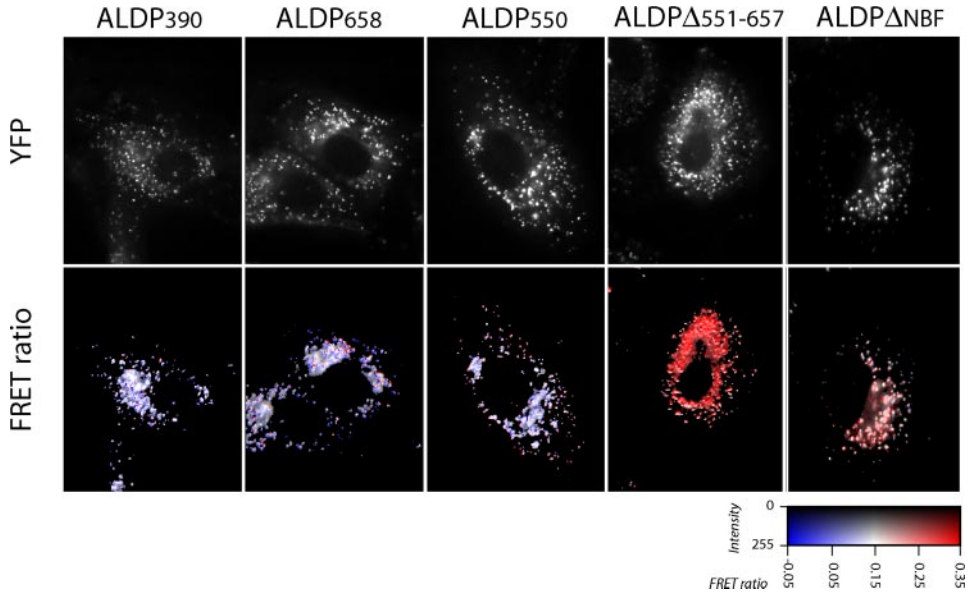

FIGURE 4. **Homodimerization of truncated ALDP proteins.** The *upper panel* shows the fluorescence distribution of YFP-labeled truncated ALDP proteins in peroxisomes of cells co-expressing the same CFP-labeled ALDP truncation mutants. Homodimerization of these ALDP truncation mutants was assessed by FRET. Their FRET ratios are presented as described in the legend to Fig. 2.

corresponding cumulative normalized distributions for these conditions are shown in *panel A*. In this analysis, only the condition ALDP/ALDP contains significantly higher FRET than the ALDP/Pex26 control. Nevertheless, the cumulative histograms also show a clear shift of the peak FRET ratio to higher values, taking an intermediate position between the ALDP/Pex26 control and the ALDP/ALDP homodimerization. The FRET probability method is not sensitive toward changes in distribution below the FRET threshold. Clearly, the choice for the threshold point at the high value of three times the standard deviation eliminates the differences that would have been registered for a lower threshold value. Therefore, the cumulative distributions were subjected to a second analysis using Kolmogorov-Smirnov (KS) statistics (37). The integrated PDFs for these conditions are shown in *panel B* of Fig. 3. These curves, known as cumulative density functions (CDFs), provide a robust estimator for distribution similarity or dissimilarity. Visually, coinciding CDFs indicate statistically identical conditions, larger separations indicate statistically significant differences. All conditions are statistically different at very low confidence levels (even lower than 1‰). Consequently, the interactions seen between ALDP with PMP70 and PMP70 with PMP70 are less pronounced than the one for ALDP with itself; nevertheless, they are relevant. KS testing returns the latter two conditions to be statistically indistinguishable from each other (*red bracket* in *panel E*). We determined an expression level for PMP70-CFP of 0.5 times the amount of endogenous cellular PMP70 in 21 cells (S.E. = 0.1) and a 6.6-fold overexpression of CFP-ALDP (S.E. = 0.9 in 16 cells). These findings indicate a lower detection sensitivity for PMP70 homodimers and PMP70-ALDP heterodimers than for ALDP homodimers.

Protein-Protein Interaction of ALDP Deletion Constructs—Because ALDP can dimerize in the peroxisomal membrane, preferentially forming homodimers, we went on to identify the protein domains that mediate these interactions. Detailed analysis for the interaction of ALDP mutant forms with the required high sensitivity was possible since FRET for homodimerization of wild type ALDP had revealed a very high efficiency. We generated various truncation mutants that lacked defined C-terminal cytoplasmic sequences including motifs like Walker A, Walker B, and the 19-mer sequence of the nucleotide binding fold (Fig. 1). We transfected cells with mutant ALDP-EYFP and co-expressed mutant ALDP-ECFP. Again, proper peroxisomal localization of the truncated fluorescence-tagged proteins was verified by co-transfection of each construct with the established peroxisomal marker ECFP-SKL or EYFP-SKL. The upper panel of Fig. 4 shows the peroxisomal localization 20–24 h after transfection of the YFP-conjugated partner for each pair of identical truncation mutants that were co-expressed. The lower panel illustrates the corresponding FRET ratios in the same scale and false color table as already shown in Fig. 2.

The mutant ALDP390 carries the largest cytoplasmic deletion covering amino acids 1–390 followed by the fluorescent proteins ECFP or EYFP (Fig. 1). ALDP390 almost exclusively contains the N-terminal half with all six transmembrane domains, but completely misses the nucleotide binding fold. This mutant allowed us to ask whether the N-terminal half of ALDP is necessary and sufficient for homodimerization. Vero cells co-expressing ALDP390-ECFP and ALDP390-EYFP showed weak FRET (Fig. 4, *left panel*) that was significantly lower than for the homodimerization of full-length ALDP (Fig. 2) but only slightly lower than for the heterodimerization of full-length ALDP with PMP70 (Fig. 2). Quantitative analysis using both 3-σ and KS statistical tests (Fig. 3, *C–E*) confirms this interpretation over multiple cells (n = 13). Statistical significance is reached at the 1% confidence level by the sensitive KS test.

Next, we used longer versions of mutant ALDP, namely ALDP550 and ALDP658. ALDP550 consists of amino acids 1 to 550 followed by either ECFP or EYFP (Fig. 1); this contains all transmembrane domains and the Walker A motif of the nucleotide binding fold. The obtained FRET ratio is slightly higher when compared with mutant ALDP390 (Fig. 3) over multiple cells (n = 9). It is statistically higher than for the ALDP/Pex26 control (5% confidence level in the 3-σ test, $\ll$1% in KS) but indistinguishable from the PMP70/ALDP association (KS = 1.4%). ALDP658 contains amino acids 1–658 followed by ECFP or EYFP (Fig. 1); this includes all six transmembrane domains and also Walker A, Walker B, and the 19-mer sequence of the nucleotide binding fold. The obtained FRET ratios are in between those for mutant ALDP390 and mutant ALDP550 over

multiple cells ($n = 11$) (Fig. 3) and are statistically identical to the values found for the PMP70/ALDP interaction (KS = 65%).

Thus, all C-terminal-truncated ALDP mutant constructs exhibit intermediate FRET values. They are lower than FRET values obtained for homodimerization of full-length ALDP, but do not reach the low FRET levels exhibited by the negative ALDP/Pex26 control. Because the extreme C terminus (amino acids 658–745) is absent in all three ALDP mutants, we assume that this protein domain influences the efficiency of the protein-protein interactions. Therefore, we fused amino acids 658–745 to the truncation mutant ALDP550 (Fig. 1). This mutant protein contains all six transmembrane domains, the Walker A motif of the nucleotide-binding fold and the extreme C terminus (amino acids 658–745). Co-expression of ALDPΔ551–657-ECFP/ALDPΔ551–657-EYFP resulted in high FRET values (Fig. 3) even surpassing the FRET levels observed in the full-length ALDP homodimerization. Both statistical tests over multiple cells ($n = 7$) revealed highly significant statistical differences with full-length ALDP. The last construct, ALDPΔNBF, lacks the complete NBF (Fig. 1). We fused the C-terminal amino acids 658–745 to the truncation mutant ALDP390 resulting in a mutant that includes all six transmembrane domains and the extreme C terminus. After transfection the ALDPΔNBF construct shows strong FRET with an overall ratio of 0.25 (Fig. 4, *right panel*) comparable with full-length ALDP. These results are supported by 3-σ and KS statistical tests over multiple cells ($n = 9$) (Fig. 3, *C–E*). They provide evidence that the extreme C-terminal part plays an important role in ALDP homodimerization and further that the nucleotide binding fold is not required.

DISCUSSION

Mutations in the gene encoding the peroxisomal membrane protein ALDP cause X-ALD, from which the protein derives its name (1, 8). X-ALD is a debilitating disease that can already manifest in early childhood and is caused by the loss or deregulation of the biological function of ALDP. ALDP is a member of the ABC transporters that most likely mediates the translocation of activated fatty acids or fatty acid substrates for catabolism by peroxisomal matrix enzymes (13, 14). A detailed understanding of the mode of operation and interaction of this class of proteins in the peroxisomal membrane is therefore important to arrive at the understanding of their molecular mechanism. Investigations using yeast two-hybrid assays and co-immunoprecipitation experiments revealed that human ALDP either forms homodimers or heterodimers with PMP70 and ALDR (28, 29, 30). In contrast, investigations using immunoprecipitated ALDP and PMP70 complexes from digitonin-solubilized mouse liver peroxisomes came to the conclusion that ALDP as well as PMP70 can only homodimerize and not heterodimerize (31). The variable, sometimes even contradicting reports on the interaction of peroxisomal ABC transporters in the literature are likely the result of differences in experimental procedures that suffer from the problems of biochemical analysis of transmembrane proteins where protein-protein interactions might be disrupted by solubilization procedures or the solubilization of membrane proteins might be incomplete leading to co-immunoprecipitation of proteins that just reside in the same membrane fragment rather than interacting with the protein of interest.

To circumvent these difficulties and limitations, we decided to investigate protein-protein interactions of ALDP in intact living cells and applied *in vivo* FRET microscopy. This approach makes it possible for us to compare different interactions in native peroxisomal membrane in the presence of all accessory proteins that safeguard adequate protein folding. The absence of FRET in the negative biological control ALDP/Pex26 shows that the overexpression of fluorescently labeled ABC transporters in Vero cells does not drive artificial interactions. This excludes a molecular crowding effect in the peroxisomal membrane, which could result in false positive FRET signals. Using live cell FRET microscopy, we were able to detect the co-existence of homomeric interactions of ALDP and PMP70, and heterodimeric interactions between ALDP and PMP70. Our observations are in good agreement with the data of other groups. Liu *et al.* (28) showed homo- as well as heterodimerization of ALDP, PMP70 and ALDR by co-immunoprecipitation experiments and yeast two-hybrid assays. In contrast to our experimental approach, they expressed proteins that lack the transmembrane domain. Smith *et al.* (29) published similar data, also showing homodimerization and heterodimerization of ALDP with PMP70 and ALDR by co-immunoprecipitation of ABC transporters synthesized by a coupled *in vitro* transcription/translation system. Tanaka *et al.* (30) demonstrated the interaction of ALDP and PMP70 together with other, as yet, unidentified proteins by immunoprecipitation of rat liver peroxisomes after incubation with 8-azido-[α-^{32}P]ATP. Intriguingly, Wouters *et al.* (38) unexpectedly detected FRET between the peroxisomal matrix protein nonspecific lipid transfer protein (nsL-TP, also called sterol carrier protein 2, SCP_2) and the ABC transporter PMP70, which was originally included as a negative control. This result was ascribed to a possible crowding effect at the membrane interface and not further investigated. In retrospect, the later verification of nsL-TP as a fatty acid carrier with a proposed role in substrate shuttling to and between peroxisomal β-oxidation pathways (39, 40) renders complex formation with PMP70 relevant. PEX26, our expression control lends credit to this possible role as we could exclude a crowding effect even inside the membrane and at high CMV-driven expression levels.

We are the first to show that the *in vitro* proposed homo- and heterodimerizations of ALDP and PMP70 also occur *in vivo*. The FRET values for the homodimerization of ALDP are higher than for PMP70 homodimerization and ALDP/PMP70 heterodimerization. ALDP heterodimerization returned FRET values that were statistically indistinguishable from those for PMP70 homodimerization. Taking into account the lower relative overexpression levels for PMP70 when compared with ALDP, it has to be noticed that the actual FRET values for PMP70 homodimerization and PMP70-ALDP heterodimerization are underestimated. This is mainly caused by the large fraction of unlabeled endogenous PMP70 that competes with CFP-labeled PMP70 for the binding of YFP-tagged acceptor protein and thus reducing the observed effective FRET signal. These findings support and complement the results of Guimarães *et al.* (31) who found homomeric interactions of ALDP and

PMP70 in digitonin-solubilized peroxisomal protein preparations, but failed to detect their heterodimers. This might be due to the high abundance of PMP70 and ALDP homodimers in the peroxisomal membrane which makes it difficult to detect the lower abundant ALDP-PMP70 heterodimers. Our data conclusively show the existence of ALDP/PMP70 heterodimers alongside their respective homodimers. Formation of heterodimers allows the regulation of transport of different cargo substances. In *Drosophila*, the uptake of precursors for the synthesis of red and brown pigments that determines eye color is controlled by various combinations of the ABC half-transporters scarlet, brown, and white, resulting in different substrate specificities (41). Analogously, the heterodimerization of ALDP with other peroxisomal ABC transporters might allow the transport of fatty acids of different chain lengths (*e.g.* very long chain fatty acids, long chain fatty acids) or classes (un/saturated fatty acids, branched chain fatty acids) or even substrates for peroxisomal β-oxidation.

Our FRET experiments with the ALDP deletion mutants demonstrate an important role of the last 87 C-terminal amino acids (amino acids 658–745) for homodimerization. In contrast, the nucleotide-binding fold is not necessary and sufficient for homodimerization as can be seen from the ALDPΔNBF construct. This is consistent with the data of Liu *et al.* (28) who showed that ALDP amino acids 361–745 are sufficient for ALDP interaction in the yeast two-hybrid assay as well as with the data of Roerig *et al.* who showed that the nucleotide binding fold is not involved in ALDP dimerization (42). In contrast to these previous studies, our deletion proteins were expressed including all six transmembrane domains. We were able to show that deletion of the complete C-terminal protein part did not fully prevent ALDP/ALDP interaction, as judged by the statistically significant residual FRET values. This strongly suggests that the transmembrane domains perform an accessory role in the stabilization of homomers.

Mutations that are causative for X-ALD occur throughout the entire *ALD* gene. In exon 10, encoding the last 81 C-terminal amino acids, to date just two mutations have been found, suggesting that this exon is of functional importance. However, Smith *et al.* (29) found that this exon has no influence on the functionality of ALDP. They transfected fibroblasts from an X-ALD patient (A626T) with an ALDP construct carrying a myc epitope replacing amino acids 693–745. This construct restored the levels of VLCFA β-oxidation to the same extent as wild-type ALDP. We cannot exclude the possibility that the C-terminal amino acids permit homodimerization by exerting a structurally stabilizing activity on the remaining fragments of the ALDP protein. In this light, either the remaining 30 AA of exon 10 or the Myc epitope or both are sufficient to restore the stability of the truncated ALDP protein. However, on the basis of our findings, we suggest that the transmembrane regions play a role in mediating or stabilizing protein interaction.

Approximately 10% of X-ALD kindred share a mutation that leads to a premature Stop codon at amino acid position 554. The mutation involves the deletion of AG at cDNA position 1415–1416 leading to a frameshift from amino acid residue Glu^{471} (fsE471). This protein lacks a functional nucleotide binding fold and is unstable and inactive (43). This suggests that stabilization of homomeric interaction by the transmembrane domain itself is not sufficient for protein stability and supports the critical role of the C-terminal part for optimal protein-protein interaction. Our data are also consistent with this conclusion as ALDPΔ551–657 and ALDPΔNBF display very high FRET intensities. In fact, these values reach or exceed those obtained for the full-length protein, suggesting that the interaction is slightly moderated by intrinsic destabilizing structures in this deletion domain.

In conclusion, our analytical *in vivo* approach performed in intact living cells expressing fluorescently labeled forms of the ABC transporters ALDP and PMP70 as well as truncation mutants of ALDP, has allowed us to confirm and consolidate previous reports on their interaction. Our findings extend beyond the verification of these interactions in a physiologically relevant setting in that they allowed the elucidation of hitherto unknown mechanistic aspects that bear direct relevance to the understanding of the mechanism of action of this class of proteins and the related human pathology: ALDP homodimers, PMP70 homodimers, and ALDP/PMP70 heterodimers exist in the peroxisomal membrane and ALDP homodimers are stabilized by their transmembrane domains.

Acknowledgments—The European Neuroscience Institute Göttingen (ENI-G) is jointly funded by the Göttingen University Medical School, the Max-Planck-Society, and Schering AG.

REFERENCES

1. Mosser, J., Douar, A. M., Sarde, C. O., Kioschis, P., Feil, R., Moser, H., Poustka, A. M., Mandel, J. L., and Aubourg, P. (1993) *Nature* **361,** 726–730
2. Kamijo, K., Taketani, S., Yokota, S., Osumi, T., and Hashimoto, T. (1990) *J. Biol. Chem.* **265,** 4534–4540
3. Gärtner, J., Moser, H., and Valle, D. (1992) *Nat. Genet.* **1,** 16–23
4. Lombard-Platet, B., Savary, S., Sarde, C. O., Mandel, J. L., and Chimini, G. (1996) *Proc. Natl. Acad. Sci. U. S. A.* **93,** 1265–1269
5. Shani, N., Jimenez-Sanchez, G., Steel, G., Dean, M., and Valle, D. (1997) *Hum. Mol. Genet.* **6,** 1925–1931
6. Holzinger, A., Kammerer, S., and Roscher, A. A. (1997) *Biochem. Biophys. Res. Commun.* **237,** 152–157
7. van Geel, B. M., Assies, J., Weverling, G. J., and Barth, P. G. (1994) *Neurology* **44,** 2343–2346
8. Moser, H., Smith, K., and Moser, A. (1995) *The Metabolic and Molecular Bases of Inherited Disease* (Scriver, C., Beaudet, A., Sly, W., and Valle, D., eds), 7th Ed., pp. 2325–2349, McGraw-Hill, New York
9. Moser, H. W. (1997) *Brain* **1207,** 1485–1508
10. Gärtner, J., Braun, A., Holzinger, A., Roerig, P., Lenard, H. G., and Roscher, A. A. (1998) *Neuropediatrics* **29,** 3–13
11. Aubourg, P., and Dubois-Dalcq, M. (2000) *Glia* **29,** 186–190
12. Guimarães, C. P., Sá-Miranda, C., and Azevedo, J. E. (2005) *J. Hum. Genet.* **50,** 99–105
13. Shani, N., and Valle, D. (1996) *Proc. Natl. Acad. Sci. U. S. A.* **93,** 11901–11906
14. Hettema, E. H., van Roermund, C. W. T., Distel, B., van den Berg M., Vilela, C., Rodrigues-Pousada, C., Wanders, R. J. A., and Tabak, H. F. (1996) *EMBO J.* **15,** 3813–3822
15. Gloeckner, C., Mayerhofer, P. U., Landgraf, P., Muntau, A. C., Holzinger, A., Gerber, J.-K., Kammerer, S., Adamski, J., and Roscher, A. A. (2000) *Biochem. Biophys. Res. Commun.* **271,** 144–150
16. Halbach, A., Lorenzen, S., Landgraf, C., Volkmer-Engert, R., Erdmann R., and Rottensteiner, H. (2005) *J. Biol. Chem.* **280,** 21176–21182
17. Landgraf, P., Mayerhofer, P. U., Polanetz, R., Roscher, A. A., and Holzinger, A. (2003) *EJCB* **82,** 401–410

18. Sacksteder, K. A., Jones, J. M., South, S. T., Li, X., Liu, Y., and Gould S. J. (2000) *J. Cell Biol.* **148,** 931–944
19. Biermanns, M., and Gärtner, J. (2001) *Biochem. Biophys. Res. Commun.* **285,** 649–655
20. Kashiwayama, y., Asahina, K., Shibata, H., Morita, M., Muntau, A. C., Roscher, A. A., Wanders, R. J. A., Shimozawa, N., Sakaguchi, M., Kato, H., and Imanaka, T. (2005) *Biochim. Biophys. Acta* **1746,** 116–128
21. Higgins, C. F. (1992) *Annu. Rev. Cell Biol.* **8,** 67–113
22. Walker, J., Saraste, M., Runswick, M., and Gay, N. (1982) *EMBO J.* **8,** 945–951
23. Gottesman, M. M., and Ambudkar, S. V. (2001) *J. Bioenerg. Biomembr.* **33,** 453–458
24. Germann, U. A., Pastan, I., and Gottesman, M. M. (1993) *Semin. Cell Biol.* **4,** 63–76
25. Riordan, J. R., Rommens, J. M., Kerem, B., Alon, N., Rozmahel, R., Grzelczak, Z., Zielinski, J., Lok, S., Plavsic, N., Chou, J. L., Drumm, M. L., Tannuzi, M. C., Collins, F. S., and Tsui, L. C. (1989) *Science* **245,** 1066–1073
26. Kelly, A., Powis, S. H., Kerr, L. A., Mockridge, I., Elliott, T., Bastin, J., Uchanska-Ziegler, A., Trowsdale, J., and Townsend, A. (1992) *Nature* **355,** 641–644
27. van Endert, P. M., Saveanu, L., Hewitt, E. W., and Lehner, P. (2002) *Trends Biochem. Sci.* **27,** 454–461
28. Liu, L. X., Janvier, K., Berteaux-Lecellier, V., Cartier, N., Benarous, R., and Aubourg, P. (1999) *J. Biol. Chem.* **274,** 32738–32743
29. Smith, K. D., Kemp, S., Braiterman, L. T., Lu, J. F., Wei, H. M., Geraghty, M., Stetten, G., Bergin, J. S., Pevsner, J., and Watkins, P. A. (1999) *Neurochem. Res.* **24,** 521–535
30. Tanaka, A. R., Tanabe, K., Morita, M., Kurisu, M., Kasiwayama, Y., Matsuo, M., Kioka, N., Amachi, T., Imanaka, I., and Ueda, K. (2002) *J. Biol. Chem.* **277,** 40142–40147
31. Guimarães, C. P., Domingues, P., Aubourg, P., Fouquet, F., Pujol, A., Jimenez- Sanchez, G., Sá-Miranda, C., and Azevedo, J. E. (2004) *Biochim. Biophys. Acta* **1689,** 235–243
32. Weller, S., Cajigas, I., Morrell, J., Obie, C., Steel, G., Gould, S. J., and Valle, D. (2005) *Am. J. Hum. Genet.* **76,** 987–1007
33. Xia, Z., and Liu, L. (2001) *Biophys. J.* **81,** 2395–2402
34. Matsumoto, N., Tamura, S., and Fujiki, Y. (2003) *Nat. Cell Biol.* **5,** 454–460
35. Gueugnon, F., Volodina, N., Et Taouil, J., Lopez, T. E., Gondcaille, C., Sequeira-Le Grand, A., Mooijer, P. A. W., Kemp, S., Wanders, R. J. A., and Savary, S. (2006) *Biochem. Biophys. Res. Commun.* **341,** 150–157
36. Esposito, A., Dohm, C. P., Kermer, P., Bähr, M., and Wouters, F. S. (2007) *Neurobiol. Dis.* **26,** 521–531
37. Demidenko, E. (2004) *Computat. Sci. Appl.* **3046,** 933–939
38. Wouters, F. S., Bastiaens, P. I. H., Wirtz, K. W. A., and Jovin, T. M. (1998) *EMBO J.* **17,** 7179–7189
39. Frolov, A., Cho, T. H., Billheimer, J. T., and Schroeder, F. (1996) *J. Biol. Chem.* **271,** 31878–31884
40. Dansen, T. B., Westerman, J., Wouters, F. S., Wanders, R. J., van Hoek, A., Gadella, T. W., and Wirtz, K. W. (1999) *Biochem. J.* **339,** 193–199
41. Ewart, G. D., Cannell, D., Cox, G. B., and Howells, A. J. (1994) *J. Biol. Chem.* **269,** 10370–10377
42. Roerig, P., Mayerhofer, P., Holzinger, A., and Gärtner, J. (2001) *FEBS Lett.* **492,** 66–72
43. Kemp, S., Pujol, A., Waterham, H. R., van Geel, B. M., Boehm, C. D., Raymond, G. V., Cutting, G. R., Wanders, R. J. A., and Moser, H. W. (2001) *Hum. Mut.* **18,** 499–515